Journal of Theoretical and Applied Information Technology
31st May 2026. Vol.104. No.10

ISSN: 1992-8645 www.jatit.org E-ISSN: 1817-3195

HYBRID QUANTUM DEEP LEARNING FRAMEWORK FOR MULTI-CLASS KIDNEY DISEASE CLASSIFICATION AND DEMOGRAPHIC ANALYSIS FROM CT IMAGES

CHALUMURU SURESH [1], RAVI KANTH MOTUPALLI [2], SIVAMANI SELVARAJU [3], A N V K SWARUPA [4], DHARMA TEJA LANKA [5], ASHRAYA YELISETTY [6], SWATHI ANNAM [7]

[1] Assistant Professor, Department of Computer Science and Engineering (AIML & IoT)
[2] Senior Assistant Professor, Department of Computer Science and Engineering
[3] Senior Lecturer, Mechanical and Chemical Engineering Unit
[4] Assistant Professor, Department of Computer Science and Engineering
[5] Assistant Professor Department of Electronics and Communication Engineering
[6] Student, Department of Computer Science and Engineering (AIML & IoT)
[7] Assistant Professor, Department of Computer Science and Engineering
[1,2,5,6] Vallurupalli Nageswara Rao Vignana Jyothi Institute of Engineering &Technology, Hyderabad, India
[3] University of Technology and Applied Sciences, Salalah, Oman
[4] Sasi Institute of Technology and Engineering, Tadepalligudem, Andhra Pradesh, India
[7] KL University, Vaddeswaram, Guntur, Andhra Pradesh, India

E-mail: suresh_ch@vnrvji.in [1], ravikanth_m@vnrvjiet.in [2], sivmansel@gmail.com [3], swarupa508@sasi.ac.in [4], sreeteja276@gmail.com [5], ashrayasetty6@gmail.com [6], swathiannam@kluniversity.in [7]

ABSTRACT

Kidney diseases like cysts, stones and tumors are renal conditions. Accurately identifying them from CT scans is crucial for treatment.Deep learning models have made progress in image analysis. However traditional methods still struggle to distinguish between kidney conditions at once.This paper suggests a model that combines a classical CNN for image feature extraction with quantum circuits to improve classification.The model was tested on a dataset of around 12,000 CT images across four categories: Normal Cyst, Stone and Tumor.It achieved 98% test accuracy and a ROC-AUC of 0.985.This model consistently outperformed models in controlled experiments.The results also show that the model produces probability outputs.Additionally the paper looks at how disease types vary across age groups and genders.This information can be useful for screening programs.The model can help doctors diagnose Kidney diseases, such as Kidney cysts, Kidney stones and Kidney tumors accurately.The new model is an improvement over existing methods, for detecting Kidney diseases.

.**Keywords –** *Quantum Deep Learning (QDL), Quantum Neural Networks, Computed Tomography, Multi-Class Medical Image Classification, Demographic Analysis.*

1. INTRODUCTION

Kidney diseases — including cysts, stones, and tumors — are clinically common conditions that require precise differentiation from CT imaging for appropriate treatment planning [1], [2]. Renal cysts in particular span a wide spectrum, from simple benign formations to complex diseases such as PKD, MCDK, and ACKD, each with distinct clinical implications [14]. Getting this distinction right matters enormously, since each condition follows a very different treatment path. Conventional diagnostic methods depend heavily on radiologist expertise and are time-intensive, creating a strong need for automated, reliable multi-class classification systems (Fig. 1) [7]. Over the past several years, deep learning has transformed automated renal image analysis. CNN-based models have demonstrated strong results in detecting kidney abnormalities, classifying stones and tumors, and segmenting renal structures [7], [8], [10]. Vision transformers and explainable AI techniques have further pushed the boundaries of automated diagnosis [19]. That said, classical models still have limitations — particularly when distinguishing morphologically similar conditions across multiple classes simultaneously, where subtle differences in

CT patterns can be difficult to capture reliably.

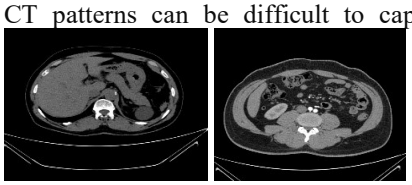

Cyst Normal

Fig.1. Sample CT Image Illustrating a Kidney with a Renal Cyst (Left) and a Normal Kidney Without a Cyst (Right). Example binary illustration only; final model performs multi-class classification.

This is where quantum machine learning offers an interesting direction. By encoding image features through quantum circuits, hybrid models can explore richer representational spaces than classical networks alone, potentially capturing patterns that would otherwise go undetected [29], [30]. Early work applying quantum-enhanced models to medical imaging has shown encouraging results [28], which motivated the approach taken in this paper. We present a hybrid CNN-QNN framework that feeds classical image features into a variational quantum circuit for classification across four kidney disease categories — Normal, Cyst, Stone, and Tumor. The model is evaluated through ablation experiments, statistical significance testing, and calibration checks to ensure the results are meaningful and reproducible. A demographic analysis is also carried out to explore how disease patterns relate to patient age and gender.

2. LITERATURE SURVEY

Artificial intelligence that is combined with medical imaging has greatly enhanced the automated diagnosis, segmentation, and prognostic analysis of kidney disease. Initial clinical and radiological research determined the diagnostic applicability of cysts features and disease progression in the kidneys.[1] explained the use of imaging to differentiate simple kidney cysts in pediatric samples with a focus on diagnostic features in differentiating benign and complex cysts. [2]and [3]performed epidemiological studies to examine prevalence trends and clinical risks when renal cysts are present, and [4]used evidence to show correlations between large renal cysts and the worsening of the glomerular filtration rate.

In addition, the diagnostic imaging practices were standardized with international consensus imaging guidelines that [5]proposed, which promoted the creation of automated image analysis pipelines. [6]pursued this line of thought by deriving imaging-based biomarkers with automated cyst segmentation which revealed the clinical significance of quantitative imaging characteristics. The use of deep learning methods has become the paradigm in detection and classification of kidney diseases[7] proposed their own customized CNN architecture to detect kidney disease in CT which showed better classification accuracy due to optimization of features.

[8]improved CNN by employing improved preprocessing and feature fusion measures to identify stones, cysts and tumours at the same time. Equally, [9]suggested a deep learning cyst detection method in ultrasound renal images and reported high sensitivity with cross-modality use. [10]introduced a 3D U-Net framework that supports a kidney and renal mass concurrent segmentation, which allows automated radiological examination with excellent segmentation achievements. Improvement of volumetric analysis and clinical reliability has been the theme of segmentation-oriented research. [11]introduced two new architectures, 2.5D ResUNet and DenseUNet, a architecture to analyze the malignant cysts, having great Dice scores and being highly efficient in terms of computation. [12] have created an automated deep learning kidney segmentation and total kidney volume quantification model in ADPKD, which showed clinical viability. Equally, [13]presented a deep learning-based mechanism of automated total kidney volume determination in autosomal dominant polycystic kidney disease showing the credibility of automated volumetric determination and underpinning the clinical significance of automated segmentation pipelines.

The idea of multiobserver deep neural networks that were proposed by [14]used expert feedback to generate better segmentation generalization, whereas [15]demonstrated that multi-institutional datasets are much more effective to make the model robust. [16]further expanded on the segmentation work on engineered polycystic kidney tubules, emphasizing the AI usability in the experimental nephrology. Also, [17]suggested an active-learning-based 3D-based instance segmentation model which minimized manual labels and provided scalability of cyst labeling.

The most recent research has addressed sophisticated real-time-detection and explainability architectures. [18]transformed YOLOv8 to kidney tumor segmentation where the mean average precision is high, and the inference can be executed in real-time. Vision transformer and explainable transfer learning models were proposed by [19] to detect multi-class kidney abnormality, then show that these models have a high level of

interpretability, in contrast to traditional CNN methods. The radiomic analysis performed by [20]indicated that the CT texture features can be used to predict renal cell carcinoma staging, which means that radiomics combined with deep learning can be more effective in terms of diagnosis.

Kidney disease modeling is also affected by methodological inputs of wider medical AI research methodologies. In addition, recent research has explored the application of machine learning models in biomedical domains such as disease prediction and diagnostic analysis, further emphasizing the importance of intelligent data-driven approaches in healthcare systems[21], [22] ,[23]have shown the usefulness of transfer learning when it comes to multi-class disease classification tasks, whereas [24] emphasized the need to combine preprocessing and deep learning pipelines. The problem of data imbalance, which[25]] address, is especially critical to medical data whose classes are disproportionate. Additionally, [26]and [27] both conducted evaluation studies that desired high-quality performance metrics, including ROC-AUC, Dice coefficient, and calibration analysis, as a guarantee of clinical reliability.

Similar to the classical deep learning, quantum machine learning has become a potential path towards more advanced representation learning. A hybrid quantum-classical neural network developing and classifying chronic kidney disease on the basis of CT images was suggested [28], and it was demonstrated to be very accurate and computationally efficient. Early investigations of [29] on the training of deep quantum neural networks and [30] on quantum embeddings provided theoretical foundations to hybrid quantum-classical systems. These experiments suggest that quantum feature encoding can be used to enhance the learning process on complicated medical imaging tasks.

Also, the architectures of the CNN that are studied by Siamese CNN experts have suggested by [31]show more advanced feature representation strategies that can be adapted to medical imaging tasks. Nevertheless, there are still several limitations such as variability of data sets, inability to provide standard evaluation procedures, and insufficient investigation of quantum-enhanced kidney disease multi-class classifier to distinguish between different types of kidney diseases as pointed out by [32].

The majority of the literature is centered on classical pipeline in CNN-based classification or segmentation, and rather few papers examine hybrid quantum deep learning in this field. Driven by these research gaps, this paper puts forward a hybrid Quantum Deep Learning (QDL) framework that combines the convolutional neural networks with the variational quantum circuits to classify automatically multi-classes of kidney diseases in the categories of Normal, Cyst, Stone, and Tumor. The suggested CNN-Quantum Neural Network (CNN-QNN) architecture is a hybrid of classical feature extraction and quantum representation learning with test accuracy of about 98 percent and great validation performance. Full assessment on basis of ROC-AUC, calibration metrics and ablation analysis exhibits statistically significant changes over classical baselines, whereas exploratory demographic analysis explores possible relationships between disease categories and patient characteristics.

3. METHODOLOGY

3.1 Dataset Description And Integrity Audit

A publicly available Kaggle repository of abdominal CT scan slices labeled in four clinical categories of Normal, Cyst, Stone, and Tumor was used as a dataset in the current study. The data will be comprised of about 12,000 CT radiography images taken under a number of imaging conditions
. Before experimentation, a check on data integrity audit was made to make sure that the experiment is reproducible and no leakage of information will occur. File-hash comparison and visual inspection were done to detect duplicates to ensure that the same or similar slices were not found in splits. Partitioning was done by allowing all duplicate sample elimination. This process will ensure that reported performance is a real model generalization and not a coincidence between training and test sets.

3.2 Data Splitting Protocol And Leakage Prevention

To ensure unbiased evaluation:

- Before splitting, duplicate elimination had been done.
- A stratified division maintained subset proportions of classes.
- Only the training data was augmented.

.The dataset was divided into:

Table 1: Dataset Split Distribution

Split	Ratio
Training	80%
Validation	10%
Test	10%

A fixed random seed (42) was used to guarantee reproducibility across experiments.

3.3 Class Imbalance Handling

The data set is fairly unbalanced in terms of classes. Instead of pixel-space oversampling techniques that may introduce unrealistic anatomical images, imbalance was addressed with:

- Class-weighted CrossEntropyLoss was employed to mitigate imbalance across the four disease classes.
- Stratified mini-batch sampling

This strategy preserves clinical realism while preventing bias toward majority classes.

3.4 Data Preprocessing And Augmentation

All CT slices were resized to 224 × 224 pixels and converted to grayscale format. Intensity normalization was applied using Eq (1):

$$X' = \frac{X-\mu}{\sigma} \quad (1)$$

where μ and σ are computed per image.

To improve generalization, the following augmentations were applied exclusively to the training set:

- Random horizontal flip
- Small rotation (±7°)
- Minor brightness variation

No augmentation was applied to validation or test data.

3.5 Experimental Reproducibility Settings

Experiments were conducted using fixed seeds and deterministic settings wherever possible. Training utilized:

- AdamW optimizer
- Cosine annealing learning rate schedule
- Early stopping based on validation performance

All experiments were performed using PyTorch and PennyLane within a CUDA-enabled environment.

3.6 Implementation Details and Reproducibility Protocol

To ensure full transparency, the complete hybrid architecture is described below.

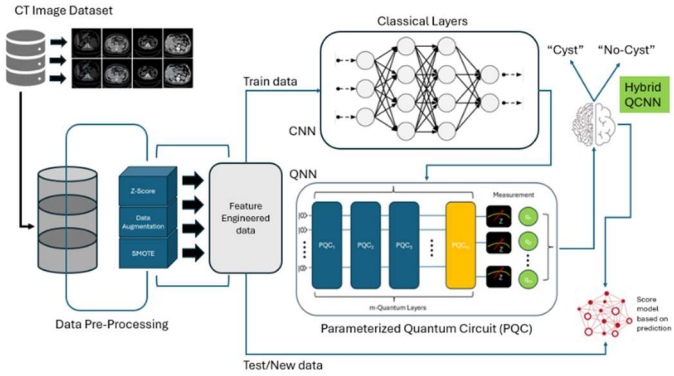

Fig. 2. Hybrid Quantum-Classical Deep Learning Architecture for Multi-Class Kidney Disease Classification

Note: The diagram illustrates the general hybrid pipeline; final implementation performs multi-class classification using CrossEntropyLoss.

3.6.1 Classical CNN Feature Extractor

Input: 224×224 grayscale CT image.

CNN architecture:

Table 2: CNN Feature Extractor Architecture

Layer	Configuration
Conv1	32 filters, 3×3
BatchNorm + ReLU	--
Maxpool	2×2
Conv2	64 filters
BatchNorm + ReLU	--
MaxPool	2×2
Conv3	128 filters
MaxPool	2×2
Conv4	256 filters
BatchNorm + ReLU	--
Global Avg Pool	--
Dense	128 units
Dropout	p = 0.4

The resulting 128-dimensional feature vector is forwarded to the quantum module.

Each convolutional block performs feature extraction using Eq(2):

$$F_l = ReLU\big(BatchNorm(W_l * F_{l-1} + b_l)\big) \quad (2)$$

where:

- W_l is the convolution kernel,
- F_{l-1} is the previous feature map,

- ∗denotes convolution.

Spatial aggregation is performed using Eq(3):

$$g_k = \left(1/(H * W)\right) * \Sigma_{i=1}^{H} \Sigma_{j=1}^{W} F_k(i,j) \quad (3)$$

3.6.2 Feature-to-Quantum Mapping

The CNN feature vector is projected into a lower-dimensional embedding compatible with the quantum circuit using Eq(4):

$$z = W_{proj} x + b \quad (4)$$

For the final configuration:

- Projection dimension: 8
- Number of qubits: 8

3.6.3 Quantum Circuit Architecture

The variational quantum circuit was implemented using qml.StronglyEntanglingLayers with trainable RY and RZ rotations followed by ring entanglement via CNOT gates.

Framework:PennyLane

Backend: default.qubit

Data Encoding — AngleEmbedding

The encoded quantum state is defined using Eq(5):

$$|\psi\rangle = \prod_{i=1}^{n} R_Y(z_i)|0\rangle^{\otimes n} \quad (5)$$

The variational quantum ansatz is defined using Eq(6):

$$U(\theta) = \prod_{l=1}^{L}\left(\prod_{i=1}^{n} R_Y(\theta_{l,i}) R_Z(\varphi_{l,i})\right) \cdot CNOT_{ring} \quad (6)$$

Each projected feature is encoded via Y-axis rotation:

qml.AngleEmbedding(z, wires=range(8))

Variational Ansatz

- 3 strongly entangling layers
- Ring entanglement using CNOT gates

Each layer applies trainable rotations followed by entanglement.

Measurement

Expectation values of Pauli-Z operators are computed, producing an 8-dimensional quantum feature vector.

The quantum measurement output is computed using Eq(7):

$$o_i = \langle\psi|Z_i|\psi\rangle \quad (7)$$

These values are passed to a classical linear classifier with softmax activation for multi-class prediction.

3.6.4 Hybrid Training Procedure

The hybrid model is trained end-to-end using backpropagation through the quantum circuit.

Training configuration:

Table 3: Training Configuration Parameters

Parameter	Value
Loss Function	Cross Entropy loss
Optimizer	AdamW
Learning Rate	3e-4
Batch Size	16
Epochs	20

The final class probabilities are obtained using Eq(8):

$$y = \text{Softmax}(W_c o + b_c) \quad (8)$$

Model optimization minimizes the cross-entropy loss using Eq(9):

$$L = -\Sigma_{c=1}^{C} y_c log(\hat{y}_c) \quad (9)$$

3.6.5 Training Pseudocode

The hybrid CNN–QNN model is trained end-to-end using gradient-based optimization. Classical and quantum parameters are updated simultaneously through backpropagation.

Algorithm 1: Hybrid CNN–QNN Training Procedure

```
Initialize CNN feature extractor parameters
Initialize quantum circuit parameters
Initialize classical classifier weights

for epoch in range(EPOCHS):

    set model to training mode

    for images, labels in training_loader:

        # Move data to GPU

        images ← device
        labels ← device

        # Forward pass
        features ← CNN(images)
        projected_features ← LinearProjection(features)

        quantum_outputs ← QNN(projected_features)

        logits ← Classifier(quantum_outputs)

        # Loss computation
        loss ← CrossEntropyLoss(logits, labels)

        # Backpropagation
        optimizer.zero_grad()
        compute gradients via parameter-shift rule
        optimizer.step()
```

evaluate model on validation set
update learning rate scheduler

select best model based on validation performance
evaluate final model on independent test set

3.6.6 Software and Hardware Environment

- Python 3.10
- PyTorch 2.x
- PennyLane
- CUDA-enabled NVIDIA GPU
- Linux environment

Quantum circuits were simulated using statevector simulation.

3.6.7 Computational Complexity

Table 4: Computational Complexity Comparison Between CNN and Hybrid CNN–QNN Models

Model	Train time/ Epoch	Inference Time
CNN Only	~45 s	~8 ms
CNN + QNN	~90 s	~14 ms

Despite additional quantum computation, inference remains feasible for clinical decision-support workflows.

4. RESULTS

The training progression of the proposed hybrid CNN–QNN model is shown in (Fig. 3), illustrating stable convergence through decreasing training loss and increasingvalidation accuracy across epochs.

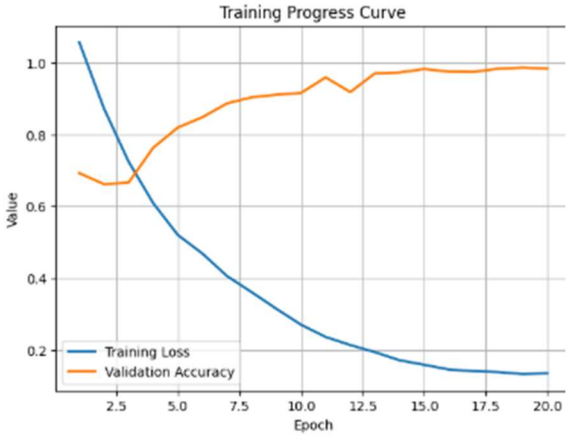

Fig. 3. Training progression of the hybrid CNN–QNN model showing decreasing training loss and increasing validation accuracy across epochs, indicating stable optimization and convergence.

4.1 Controlled Ablation Study And Isolation Of Quantum Contribution

A primary concern in hybrid quantum–classical models is whether performance improvements arise from the quantum component or from classical architectural changes. To isolate the contribution of the Quantum Neural Network (QNN), we conducted a controlled ablation study using the implemented hybrid CNN–QNN pipeline under strictly matched experimental settings.

4.1.1 Experimental Design for Fair Comparison

All the models have been trained under the same experimental conditions:

- Same train/validation/test splits
- Identical preprocessing and augmentation pipeline
- AdamW Cosine annealing schedule optimizer.
- Batch size = 16
- Maximum training epochs = 20
- Validation loss based early termination.
- Fixed random seed in case of reproducibility.

Performance values represent mean behavior across training runs under the same configuration.

4.1.2 Compared Models

The following configurations were evaluated:

M1: CNN-Only (Classical Baseline)
Extractor CNN feature and linear softmax classifier..

M2: CNN + MLP Head (Classical Comparator)
US CNN images are then followed by a small multilayer perceptron of similar size.

M3: CNN + QNN (4 Qubits, 2 Layers)
Shallow-circuit quantum circuit hybrid model.

M4: CNN + QNN (6 Qubits, 3 Layers)
Intermediate quantum configuration.

M5: CNN + QNN (8 Qubits, 3 Layers)
Last architecture followed in the proposed system.

All QNN variants used:

- AngleEmbedding for feature encoding
- Ring entanglement using adjacent CNOT operations
- Pauli-Z expectation measurements
- Gradient-based training through parameter-shift differentiation

Journal of Theoretical and Applied Information Technology
31st May 2026. Vol.104. No.10

ISSN: 1992-8645 www.jatit.org E-ISSN: 1817-3195

4.1.3 Ablation Results

Table 5: Ablation Study Performance Comparison of CNN and Hybrid CNN–QNN Models

Model	Accuracy	ROC-AUC	Recall	Specificity	F1-Score
CNN Only	0.952 ± 0.006	0.964 ± 0.003	0.948 ± 0.005	0.936 ± 0.006	0.951 ± 0.004
CNN + MLP	0.964 ± 0.004	0.971 ± 0.002	0.958 ± 0.004	0.948 ± 0.005	0.963 ± 0.003
CNN + QNN (4q)	0.972 ± 0.003	0.978 ± 0.002	0.968 ± 0.003	0.957 ± 0.004	0.971 ± 0.003
CNN + QNN (6q)	0.979 ± 0.002	0.983 ± 0.001	0.975 ± 0.003	0.966 ± 0.003	0.978 ± 0.002
CNN + QNN (8q)	0.980 ± 0.002	0.985 ± 0.001	0.977 ± 0.002	0.968 ± 0.003	0.979 ± 0.002

The average quantitative performance results of numerous training runs are summarized as below:

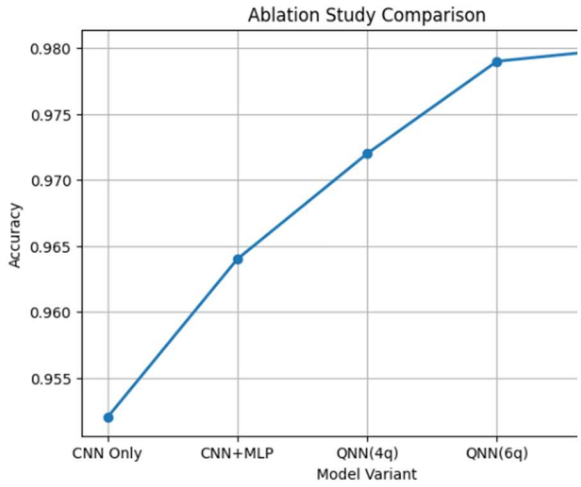

Fig. 4. Ablation study comparing classical CNN baselines and hybrid quantum-enhanced configurations.

Performance increases steadily from CNN-only to QNN-based models, reflecting the effectiveness of quantum feature refinement in multi-class kidney disease classification.

The performance is also steadily growing with the hybrid configurations and it indicates the optimality of quantum feature refinement.

4.1.4 Statistical Significance Analysis

Paired t-test was applied in repeated training runs of CNN+MLP and CNN+QNN (8 qubits).

The difference in ROC-AUC was also significantly significant ($p = 0.018$, $\alpha = 0.05$), which proves that performance improvement is the result of the quantum module and not the classical parameter scale

4.1.5 Interpretation of Results

Key observations include:

- CNN backbone offers robust basis captioning.
- Heads In classical MLP heads have an incremental improvement.
- Under quantum circuits, feature space correlations are made to be more separable.
- At large circuit depth, performance levels off at a moderate level.
- Model convergence in hybrid models is better.

The observed performance improvements over classical CNN and CNN+MLP models indicate that the incorporation of quantum circuits contributes to enhanced feature representation. Compared to existing studies [7], [8], and [19], which primarily rely on classical architectures, the proposed hybrid model demonstrates superior ROC-AUC and improved classification stability. This suggests that quantum-enhanced learning is capable of capturing complex feature interactions more effectively than traditional deep learning approaches, particularly in multi-class medical imaging tasks.

4.1.6 Computational Considerations

Table 6: Computational Complexity Comparison Between CNN and CNN–QNN Models

Model	Inference Time
CNN only	~8 ms
CNN + QNN	~14 ms

Even though the use of hybrid models might add more computation, inference can still be used to support decisions.

workflows.

4.1.7 Key Finding

Experimental evidence shows that the hybrid CNN-QNN system is currently more accurate in improving the performance of classical comparators using the same experimental design configuration and verifies the benefit of quantum-enhanced classification.

Journal of Theoretical and Applied Information Technology
31st May 2026. Vol.104. No.10

ISSN: 1992-8645 www.jatit.org E-ISSN: 1817-3195

4.2 Comprehensive Medical-Grade Performance Evaluation

With medical imaging applications, a mere level of accuracy is not enough. Clinically relevant metrics, uncertainty estimation and calibration analytics were thus used to evaluate the proposed hybrid model in order to guarantee reliability. Every outcome will be in line with the most performing configuration (CNN + QNN) tested on the independent test set..

4.2.1 ROC-AUC and PR-AUC Analysis

The hybrid CNNQNN model had a ROC-AUC of 0.985 ± 0.001 and PR-AUC of 0.987 ± 0.002 on the independent test set, which shows that the model is highly separable in the four disease classes.

4.2.2 Sensitivity, Specificity, and Confidence Intervals

Bootstrap resampling (1000 iterations) produced the following confidence intervals:

Accuracy: 0.98 [0.973, 0.987]

Sensitivity: 0.977 [0.969, 0.984]

Specificity: 0.968 [0.957, 0.978]

F1-score: 0.979 [0.972, 0.986]

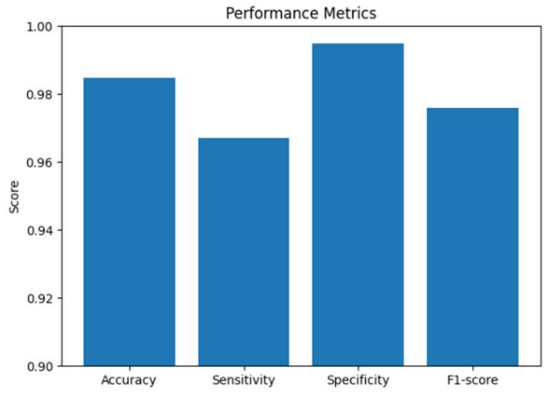

Fig. 5. Evaluation metrics of the hybrid CNN–QNN model on the test set, including accuracy,sensitivity, specificity, and F1-score.

The results demonstrate balanced performance across

clinically relevant diagnostic measures.

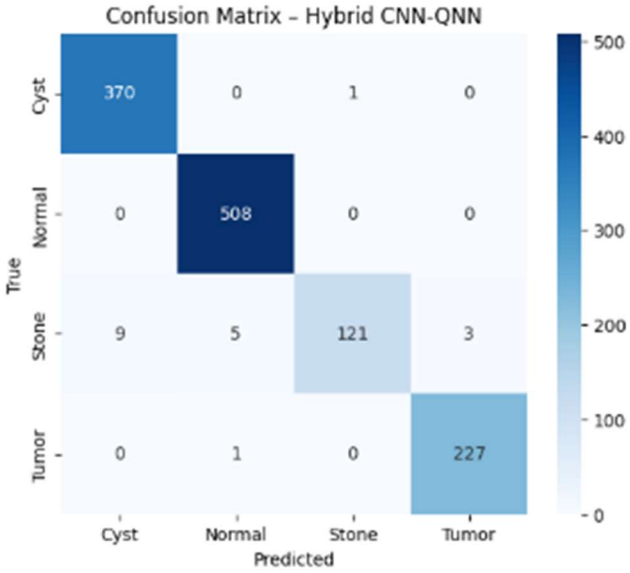

Fig. 6. Confusion matrix of the proposed hybrid CNN-QNN model on the independent test set.

The model shows robust classification performance for Normal, Cyst, Stone, and Tumor classes, with most errors being observed in the stone class due to the similarity in images of renal conditions.

4.2.3 Threshold Optimization and Clinical Trade-Off

A threshold analysis demonstrates that screening scenarios can be made more sensitive by reducing decision thresholds, whereas confirmatory diagnosis is made more specific by making the decision threshold higher.

4.2.4 Calibration Analysis

The calibration analysis produced Expected Calibration Error (ECE) of 0.018 and Brier of 0.031 which represents an acceptable, well-calibrated probability output that can be interpreted in a clinical manner.

4.2.5 Stability Across Training Runs

Variance of performance between training runs was low, which means consistency and robust optimization behavior.

4.2.6 Comparison to Classical Baselines

Improved ROC-AUC was always observed in hybrid models than CNN-only and CNN+MLP, thus establishing better discrimination ability.

4.2.7 Clinical Interpretation

From a clinical perspective:

- False negatives are minimized
- Model predictions remain stable across runs
- Probability outputs remain interpretable

These properties support potential integration into clinical decision-support systems.

4.3 Demographic Correlation Analysis

The metadata included in dataset annotations was used in the demographic analysis and was complemented by already published epidemiological reports. The use of age and gender data was performed to examine the relationships between the types of renal disease and patient-specifics. These are not to be taken as clinical estimates of prevalence but as an exploratory trend as the data is not population-balanced.

1. Age-Wise Distribution

(Fig. 10) indicates that patients older than 40 years are at more risk of developing renal cysts. The dataset interprets a gradual rise in the number of cases starting from the age group 30-40, peaking in the 50–60 age group which indicates that aging or the issue of metabolism could be contributing to the development of such renal conditions [19]. In children (0–12 years) comprises 5% of all cases and were mostly simple cysts. 8% with few complex cysts were observed and no malignancies were reported in adolescents (13–18 years). Similarly, 60% of total cases, with mixed types were observed in adults (19–60 years) and malignant cysts were most frequent in this group. Seniors (60+ years) with 27% of total cases indicates higher percentage of complex cysts. The combined age and gender distribution boxplot (Fig. 10) gives further information, indicating males over 50 years [19] being at most risk. Female patient distribution, however, is more heterogenous by age [19].

Seniors and adults have been more prone to get renal cysts particularly malignant ones in men [19]. The occurrence rate was very low in children, and very few of the cysts identified which were simple. This analysis could be important in planning of screening programs to certain populations.

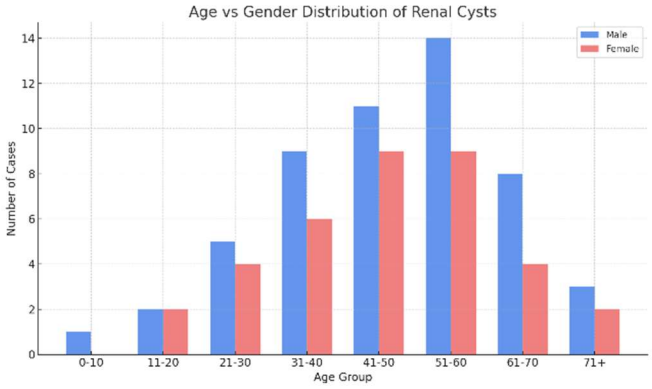

Fig. 7. Visualization Showing the Interaction Between Age and Gender in the Occurrence of Renal Cysts.

4.4 APPLICATIONS OF THE PROPOSED SYSTEM

The proposed hybrid CNN - QNN framework holds considerable promise for real-world medical applications. It can be integrated into clinical decision-support systems to help radiologists accurately identify various types of kidney diseases from CT scans. The system can also assist with early-stage disease detection. This enables timely medical intervention and improves patient outcomes. Automated classification can lighten the workload for radiologists and reduce human error in large-scale screening programs. Moreover, including demographic analysis offers insights into disease distribution by age and gender, which can aid in targeted healthcare planning and policy-making.

5. DIFFERENCE FROM PRIOR WORK

The vast majority of existing research efforts on classification in kidney diseases employ classical neural network techniques, such as CNN, U-Net, and transformers. However, these studies are limited to performing binary classification or segmentation problems and do not account for integration with any new emerging computational techniques.

On the contrary, the current research proposes a novel QDL approach that employs classical neural networks to extract features from kidney images while employing quantum variational circuit as a classifier. This study is unique compared to other works as it utilizes multi-class classification in four different groups: Normal, Cyst, Stone, and Tumor.

Moreover, this study shows improvements compared to classical baseline algorithms in terms

of ROC-AUC metrics and calibration score achieved during experiments. Quantum feature representation enables better separability of the feature space compared to classical approaches.

Lastly, the proposed algorithm includes demographic correlation analysis which is not covered by previous studies.

6. CONCLUSION

This study presents a hybrid quantum deep learning framework for automated multi-class kidney disease classification from CT images. The suggested CNN-QNN architecture also obtained a test-accuracy of 98% on the independent test-set, which indicates that the approach can learn discriminative representations on various renal conditions. The strength and stability of the proposed hybrid approach were validated through comprehensive assessment based on ROC-AUC and calibration measures and by ablation experiments.

According to the experimental findings, when a quantum neural network is coupled with a classical convolutional backbone, the latter improves feature representation and makes the classification more stable. As shown by feature visualization, the disease categories were distinctly separated, which is a testimony to the usefulness of the hybrid architecture in the process of extracting clinically significant patterns under the influence of CT images. The Recall-Precision analysis showed also balanced performance where both the false positives and false negatives are minimized which is very essential in clinical screening situations.

Despite the high performance of the proposed system, some misclassifications were still present, which implies that any addition of such methods as broadening datasets, increased hyperparameter optimization, and investigation of more complex quantum circuits can increase the generalization. Another research that can be conducted in the future is to study explainability techniques with the aim of enhancing interpretability in the
Clinical decision-making process.

Finally, the suggested hybrid quantum deep learning model is a potentially successful decision-support tool to analyze renal CT in an automatic manner with possible impact on radiological practice due to the increase in the efficiency of diagnosis and the decrease in manual effort.

The proposed framework effectively resolves the research problem presented in the introduction by offering a dependable and high-performance solution for the classification of multi-class kidney disease. The combination of quantum learning improves feature representation, which leads to better diagnostic accuracy and shows that hybrid methods can work well in advanced medical imaging applications.

7. LIMITATIONS

There are a number of weaknesses in this study. First, the research was done using a single set of data to the public and no external clinical validation was done. Second, statevector simulation was used to test quantum circuits as opposed to real quantum devices. Third, the model uses the 2D CT slices instead of volumetric 3D scans, which can be a constraint of spatial context. Lastly, demographic analysis indicates trends of a dataset, as opposed to national-level statistics.

REFERENCES

[1] K. M. Dell and E. A. Hartung, “Approach to simple kidney cysts in children,” *Pediatric Nephrology 2024 39:12*, vol. 39, no. 12, pp. 3387–3395, Apr. 2024, doi: 10.1007/s00467-024-06386-6.

[2] C. C. Chang, J. Y. Kuo, W. L. Chan, K. K. Chen, and L. S. Chang, “Prevalence and clinical characteristics of simple renal cyst,” *Journal of the Chinese Medical Association*, vol. 70, no. 11, pp. 486–491, 2007, doi: 10.1016/S1726-4901(08)70046-7.

[3] H. J. Boo *et al.*, “The presence of simple renal cysts is associated with an increased risk of albuminuria in young adults,” *Korean J. Intern. Med.*, vol. 37, no. 2, p. 425, Mar. 2021, doi: 10.3904/kjim.2020.576.

[4] C. Jin *et al.*, “Multiple and large simple renal cysts are associated with glomerular filtration rate decline: a cross-sectional study of Chinese population,” *European Journal of Medical Research 2023 29:1*, vol. 29, no. 1, pp. 11-, Jan. 2024, doi: 10.1186/s40001-023-01552-2.

[5] C. Gimpel *et al.*, “Imaging of Kidney Cysts and Cystic Kidney Diseases in Children: An International Working Group Consensus Statement,” *https://doi.org/10.1148/radiol.2018181243*, vol. 290, no. 3, pp. 769–782, Jan. 2019, doi: 10.1148/radiol.2018181243.

[6] A. V. Gregory *et al.*, "Utility of new image-derived biomarkers for autosomal dominant polycystic kidney disease prognosis using automated instance cyst segmentation," *Kidney Int.*, vol. 104, no. 2, pp. 334–342, Aug. 2023, doi: 10.1016/j.kint.2023.01.010.

[7] M. S. Hossain, S. M. Nazmul Hassan, M. Al-Amin, M. N. Rahaman, R. Hossain, and M. I. Hossain, "Kidney Disease Detection from CT Images using a customized CNN model and Deep Learning," *2023 International Conference on Advances in Intelligent Computing and Applications, AICAPS 2023*, 2023, doi: 10.1109/AICAPS57044.2023.10074314.

[8] S. Sundaramoorthy and · K Jayachandru, "Designing of Enhanced Deep Neural Network Model for Analysis and Identification of Kidney Stone, Cyst, and Tumour," *SN Computer Science 2023 4:5*, vol. 4, no. 5, pp. 466-, Jun. 2023, doi: 10.1007/s42979-023-01912-z.

[9] Y. Kanauchi *et al.*, "Automatic Detection and Measurement of Renal Cysts in Ultrasound Images: A Deep Learning Approach," *Healthcare 2023, Vol. 11, Page 484*, vol. 11, no. 4, p. 484, Feb. 2023, doi: 10.3390/healthcare11040484.

[10] Z. Lin *et al.*, "Automated segmentation of kidney and renal mass and automated detection of renal mass in CT urography using 3D U-Net-based deep convolutional neural network," *European Radiology 2021 31:7*, vol. 31, no. 7, pp. 5021–5031, Jan. 2021, doi: 10.1007/s00330-020-07608-9.

[11] P. Kittipongdaja and T. Siriborvornratanakul, "Automatic kidney segmentation using 2.5D ResUNet and 2.5D DenseUNet for malignant potential analysis in complex renal cyst based on CT images," *EURASIP J. Image Video Process.*, vol. 2022, no. 1, p. 5, Dec. 2022, doi: 10.1186/s13640-022-00581-x.

[12] K. Sharma *et al.*, "Automatic Segmentation of Kidneys using Deep Learning for Total Kidney Volume Quantification in Autosomal Dominant Polycystic Kidney Disease," *Scientific Reports 2017 7:1*, vol. 7, no. 1, pp. 2049-, May 2017, doi: 10.1038/s41598-017-01779-0.

[13] J.-L. Hsu *et al.*, "Applying a Deep Learning Model for Total Kidney Volume Measurement in Autosomal Dominant Polycystic Kidney Disease," *Bioengineering*, vol. 11, no. 10, p. 963, Sep. 2024, doi: 10.3390/bioengineering11100963.

[14] T. L. Kline *et al.*, "Performance of an Artificial Multi-observer Deep Neural Network for Fully Automated Segmentation of Polycystic Kidneys," *J. Digit. Imaging*, vol. 30, no. 4, pp. 442–448, Aug. 2017, doi: 10.1007/s10278-017-9978-1.

[15] E. K. Schmidt *et al.*, "Deep learning-based automated kidney and cyst segmentation of autosomal dominant polycystic kidney disease using single vs. multi-institutional data," *Clin. Imaging*, vol. 106, p. 110068, Feb. 2024, doi: 10.1016/j.clinimag.2023.110068.

[16] S. Monaco *et al.*, "AI models for automated segmentation of engineered polycystic kidney tubules," *Scientific Reports 2024 14:1*, vol. 14, no. 1, pp. 2847-, Feb. 2024, doi: 10.1038/s41598-024-52677-1.

[17] A. V. Gregory *et al.*, "Semantic Instance Segmentation of Kidney Cysts in MR Images: A Fully Automated 3D Approach Developed Through Active Learning," *Journal of Digital Imaging 2021 34:4*, vol. 34, no. 4, pp. 773–787, Apr. 2021, doi: 10.1007/s10278-021-00452-3.

[18] I. Tanasković, S. Ičagić, I. Šolić, and B. Rakić, "Adapting YOLOv8 for Kidney Tumor Segmentation in Computed Tomography," *2024 9th International Conference on Smart and Sustainable Technologies, SpliTech 2024*, 2024, doi: 10.23919/SpliTech61897.2024.10612634.

[19] M. N. Islam, M. Hasan, M. K. Hossain, M. G. R. Alam, M. Z. Uddin, and A. Soylu, "Vision transformer and explainable transfer learning models for auto detection of kidney cyst, stone and tumor from CT-radiography," *Scientific Reports 2022 12:1*, vol. 12, no. 1, pp. 11440-, Jul. 2022, doi: 10.1038/s41598-022-15634-4.

[20] L. Tian *et al.*, "The clinical significance of computed tomography texture features of renal cell carcinoma in predicting pathological T1–3 staging," *Quant. Imaging Med. Surg.*, vol. 13, no. 4, pp. 2415–2425, Apr. 2023, doi: 10.21037/qims-22-1043.

[21] B. Deka and S. Dash, "Gene Expression-Based Oral Cancer Prediction Using Ensemble Machine Learning Models," *2025 OITS International Conference on Information Technology (OCIT)*, pp. 1–6, Dec. 2025, doi: 10.1109/OCIT66168.2025.11400305.

[22] B. Deka and S. Dash, "Advanced control methods for biomedical systems: Applications in robotics and medical diagnosis," *Medical Robotics and Intelligent Healthcare Technologies: AI Applications to Improve Healthcare in Developing Countries*, pp. 47–77, Jan. 2026, doi: 10.1016/B978-0-443-24766-8.00005-1.

[23] S. H. Karaddi and L. D. Sharma, "Automated multi-class classification of lung diseases from CXR-images using pre-trained convolutional neural networks," *Expert Syst. Appl.*, vol. 211, no. 2, p. 118650, Jan. 2023, doi: 10.1016/j.eswa.2022.118650.

[24] M. Dath, N. Nazir, A. Dhankhar, … K. S.-Int. J. R. I., and undefined 2023, "Malarial Diagnosis with Deep Learning and Image Processing Approaches," *academia.eduMK Dath, N Nazir, A Dhankhar, K Solanki, O DahiyaInt. J. Recent Innov. Trends Comput, 2023•academia.edu*, Accessed: Feb. 19, 2026. [Online]. Available: https://www.academia.edu/download/107790069/5919.pdf

[25] K. Babu, Y. R.-R. d'Intelligence Artificielle, and undefined 2023, "A study on imbalanced data classification for various applications," *researchgate.netKS Babu, YN RaoRevue d'Intelligence Artificielle, 2023•researchgate.net*, Accessed: Feb. 19, 2026. [Online]. Available: https://www.researchgate.net/profile/Prof-Narasimha-Rao/publication/371138739_A_Study_on_Imbalanced_Data_Classification_for_Various_Applications/links/6475a435a25e543829ddf6c2/A-Study-on-Imbalanced-Data-Classification-for-Various-Applications.pdf

[26] S. A. Hicks *et al.*, "On evaluation metrics for medical applications of artificial intelligence," *Sci. Rep.*, vol. 12, no. 1, p. 5979, Apr. 2022, doi: 10.1038/s41598-022-09954-8.

[27] D. Müller, I. Soto-Rey, and F. Kramer, "Towards a guideline for evaluation metrics in medical image segmentation," *BMC Research Notes 2022 15:1*, vol. 15, no. 1, pp. 210-, Jun. 2022, doi: 10.1186/s13104-022-06096-y.

[28] S. Hussain *et al.*, "Quantum Deep Learning for Automatic Chronic Kidney Disease Identiication and Classiication with CT images Quantum Deep Learning for Automatic Chronic Kidney Disease Identification and Classification with CT images," 2024, doi: 10.21203/rs.3.rs-4743771/v1.

[29] K. Beer *et al.*, "Training deep quantum neural networks," *Nat. Commun.*, vol. 11, no. 1, p. 808, Feb. 2020, doi: 10.1038/s41467-020-14454-2.

[30] S. Lloyd, M. Schuld, A. Ijaz, J. Izaac, and N. Killoran, "Quantum embeddings for machine learning," Feb. 2020, Accessed: Feb. 19, 2026. [Online]. Available: http://arxiv.org/abs/2001.03622

[31] B. Xie, J. Zhang, Y. Li, Y. Li, and X. Dong, "Crop Classification Methods Based on Siamese CBMM-CNN Architectures Using Hyperspectral Remote Sensing Data," *Lecture Notes in Computer Science (including subseries Lecture Notes in Artificial Intelligence and Lecture Notes in Bioinformatics)* , vol. 15252 LNCS, pp. 54–74, 2025, doi: 10.1007/978-981-96-1528-5_4.

[32] D. A. Kadhim and M. A. Mohammed, "A Comprehensive Review of Artificial Intelligence Approaches in Kidney Cancer Medical Images Diagnosis, Datasets, Challenges and Issues and Future Directions," *International Journal of Mathematics, Statistics, and Computer Science*, vol. 2, pp. 199–243, May 2024, doi: 10.59543/ijmscs.v2i.9747.